Soft Matter

Accepted Manuscript

ROYAL SOCIETY OF CHEMISTRY

www.rsc.org/softmatter

ARTICLE TYPE www. rsc.org/xxxxxx | XXXXXXXX

Force-dependent persistence length of DNA-intercalator complexes measured in single molecule stretching experiments

R. F. Bazoni,[a] C. H. M. Lima,[a] E. B. Ramos,[a] and M. S. Rocha*[a]

Received Xth XXXXXXXXXX 20XX, Accepted Xth XXXXXXXXX 20XX
First published on the web Xth XXXXXXXXXX 200X
DOI: 10.1039/b000000x

By using optical tweezers with an adjustable trap stiffness, we have performed systematic single molecule stretching experiments with two types of DNA-intercalator complexes, in order to investigate the effects of the maximum applied forces on the mechanical response of such complexes. We have explicitly shown that even in the low-force entropic regime the persistence length of the DNA-intercalator complexes is strongly force-dependent, although such behavior does not occur for bare DNA molecules. We discuss the possible physicochemical effects that can lead to such results. In particular, we propose that the stretching force can promote partial denaturation on the highly distorted double-helix of the DNA-intercalator complexes, which interfere strongly in the measured values of the persistence length.

1 Introduction

The study of DNA interactions with ligands such as drugs or proteins is an interdisciplinary field important both in the investigation of many intracellular processes as well as in applications on the health sciences, especially in cancer chemotherapies and gene therapies. From the early 90's, the advent of single molecule techniques such as optical and magnetic tweezers has allowed one to investigate these interactions by manipulating and stretching single DNA-ligand complexes, since the mechanical response of these complexes usually changes upon ligand binding. In fact, along the past years various approaches were developed in order to deduce the ligand binding mode(s) and to extract physicochemical information of the interaction from mechanical data obtained by performing single molecule stretching on DNA-ligand complexes [1–20].

Although nowadays the mechanical behavior of bare DNA molecules is well understood, the mechanics of DNA-ligand complexes is still a topic with many contradictory results in the literature, especially when comparing data obtained from single molecule stretching techniques with those obtained from typical ensemble-averaging techniques. In single molecule stretching experiments performed with optical or magnetic tweezers, each individual DNA-ligand complex is stretched from its equilibrium configuration in solution to an approximately straight configuration, and the mechanical properties are determined by fitting the force × extension curve to some theoretical model of polymer elasticity. In ensemble-averaging techniques such as dynamic light scattering, viscosimetry and gel electrophoresis, otherwise, the complexes are not mechanically manipulated and the mechanical properties are deduced from the conformation of a set of many molecules.

Intercalators are well known DNA binding drugs much used in various types of cancer chemotherapies. The binding of these drugs introduce strong structural perturbations on the double-helix structure, increasing the DNA contour length and unwinding the double-helix by a certain angle per intercalated molecule [7,21–25]. Despite the large use of intercalators in cancer chemotherapies and the large number of studies concerning the interactions of these drugs with DNA, there are still some contradictory results in the literature about the effects of these compounds on the DNA persistence length. In fact, there are a some works such as the ones of Sischka *et al.* [7] and Husale *et al.* [8], performed with optical tweezers; Maaloum *et al.* [26], performed with atomic force microscopy (AFM); Murade *et al.* [27], performed with optical tweezers and fluorescence microscopy; and Lipfert *et al.* [28], performed with magnetic tweezers, which have reported a decrease on the persistence length of DNA complexes formed with intercalators. On the other hand there are works that report an increase on the persistence length of DNA-intercalator complexes upon drug binding, such as those by Reinert *et al.* [29], performed with viscosimetry; Quake *et al.* [30], performed with optical tweezers and fluorescence microscopy; Berge *et al.* [31], performed with AFM; and the works from the group of K. Yoshikawa [32–35] all performed with fluorescence microscopy. Finally, there are works that have reported that intercalators in general firstly increase the DNA persistence length for low ligand concentrations, but can decrease this parameter for high ligand concentrations. As examples, we cite the works of Tessmer *et*

[a] *Laboratório de Física Biológica, Departamento de Física, Universidade Federal de Viçosa. Viçosa, Minas Gerais, Brazil. Fax: 55-31 3899-2483 ; Tel: 55-31 3899-3399; E-mail: marcios.rocha@ufv.br*

al.[6], performed with optical tweezers, Cassina *et al.*[36] and Kaji *et al.*[37], performed with AFM; and the works of our group[12,13,19,20], all performed with optical tweezers. Therefore, given the current state of knowledge on the subject, it is clear that a rigorous systematic investigation is needed in order to understand such discrepant results.

As a starting point, it is important to note that most works that have used non-stretching experimental techniques have concluded that the persistence length of DNA-intercalator complexes increases upon drug binding[29,30,32–35]. Most of the contradictory results, otherwise, were obtained from experiments performed with typical DNA stretching techniques, such as optical and magnetic tweezers[6–8,12,13,19,20,27,28].

In order to clarify these contradictory results, in this work we use optical tweezers to perform systematic stretching experiments with DNA complexes formed with two intercalators, Doxorubicin (doxo) and Ethidium Bromide (EtBr), by varying the tweezers' trap stiffness. The goal is to verify the effects of the maximum applied forces on the mechanical properties of the DNA-drug complexes. Doxo is an anthracycline antibiotic largely employed in chemotherapies for treating some types of leukemias, sarcomas, lymphomas, etc. EtBr, on the other hand, is a fluorescent dye much used to stain the DNA molecule in gel electrophoresis and other methods of nucleic acids separation. In Fig. 1 we show the chemical structure of both compounds. At near physiological conditions ([NaCl] $\sim$ 150 mM, pH $\sim$ 7.4) doxo intercalates in the DNA molecule with an equilibrium binding association constant of about $\sim 10^8$ M^{-1}, occupying 2.5 to 3 base-pairs in average[38,39]. EtBr, on the other hand, intercalates with an equilibrium binding constant of about $\sim 10^5$ M^{-1}, occupying 2.0 to 2.5 base-pairs[12,40].

Here the experiments were performed stretching the complexes up to three different values of the maximum force: $\sim$ 6 pN, $\sim$ 10.5 pN and $\sim$ 15 pN. Basically we have found that, the higher the maximum applied force, the lower the persistence length obtained from single molecule stretching. We discuss and interpret the results mainly in terms of partial DNA denaturation induced by the stretching force on the highly distorted double-helix of the DNA-intercalator complexes, which interfere strongly in the measured values of the persistence length.

2 Materials and Methods

2.1 Sample preparation

In this work the samples consist of λ-DNA molecules (New England Biolabs) end-labeled with biotin attached by one end to a streptavidin-coated bead of 3 μm diameter (Bangs Labs) and by the other end to a streptavidin-coated coverslip (Xenopore Corp.). The surrounding solution is a Phosphate Buffered Saline (PBS) buffer with pH = 7.4 and [NaCl] = 140 mM. The sample chamber consist of an o-ring glued in the coverslip surface, which contains the working solution. The DNA base-pair concentration used in all experiments was C_{bp} = 2.4 μM. The surrounding buffer solution, and consequently the drug concentration in the sample, can be easily changed during the experiments by using micropipettes.

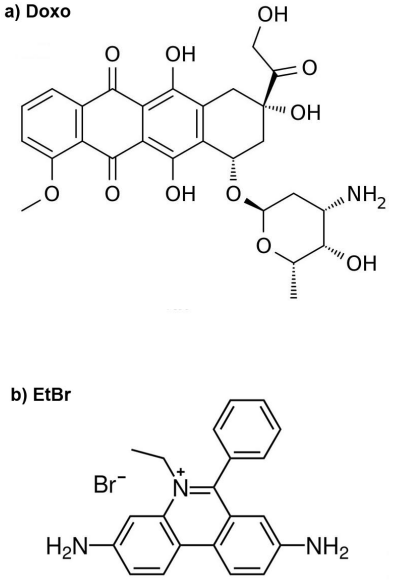

Fig. 1 Chemical structure of the two intercalators used: a) Doxorubicin (doxo) and b) Ethidium Bromide (EtBr).

2.2 Optical tweezers setup

The optical tweezers consist of a 1064 nm ytterbium-doped fiber laser with a maximum output power of 5.8 W (IPG Photonics) mounted on a Nikon Ti-S inverted microscope with a 100$\times$ N.A. 1.4 objective. As mentioned before, we have performed measurements with three different values for the trap stiffness κ: (6.2 $\pm$ 0.3) pN/μm, (10.9 $\pm$ 0.5) pN/μm and (15.5 $\pm$ 0.8) pN/μm. This parameter was changed by varying the laser output power and/or using neutral density filters in the optical path. Each value of κ was obtained by calibrating the tweezers with two independent methods using free beads (without attached DNA) in solution: indirect Stokes force calibration and by analyzing the Brownian fluctuations of the bead in the potential well of the tweezers[41]. Once calibrated, the tweezers can be used to trap a polystyrene bead attached to a DNA molecule and the stretching experiments can be started.

2.3 Stretching experiments

The DNA molecules are stretched by moving the microscope stage and consequently the coverslip with controlled velocity by using a piezoelectric device (PINano P-545, Physik Instrumente). Simultaneously, we monitor the changes on the bead position in the potential well of the tweezers, $x(t)$, by videomicroscopy. Therefore, the stretching force can be determined as $F(t) = \kappa x(t)$, and t is converted to the DNA extension x_{DNA} by multiplying by the velocity of the coverslip. To extract the persistence and contour lengths, we fitted the experimental force × extension data to the Marko-Siggia Worm-Like Chain (WLC) model[42].

In order to change the maximum value of the force applied to the DNA molecules, the trap stiffness κ of the tweezers is varied. This approach has been proved better than simply stopping the stretching experiments at different points, because it allows one to measure similar bead displacements in the optical potential well for different maximum forces, thus minimizing errors due the to bead displacement measurements. Such displacements can be very small in the entropic regime if the trap stiffness is too high, thus increasing the error in the measurement of the force.

Another fundamental issue that was addressed here was to fit only the experimental force × extension data that is rigorously within the harmonic region of optical potential well. In fact, considerable variations on the trap stiffness usually occur for high bead displacements, because it can enter in the anharmonic regions of the optical potential[43,44]. To avoid such effect, which can lead to wrong results due to calibration mismatch, we have previously determined for each κ which are the maximum allowed forces that can be used in the fitting process. Such forces depend on the particular characteristics of each particular experimental setup that determine the shape of the optical potential (bead size and refractive index, bead distance from coverslip, laser wavelength and mode, etc)[43]. For our current setup, the maximum bead displacement that can be used to fit the experimental force × extension data is ~ 0.32 μm independent of the trap stiffness used, which corresponds to 9.3 pixels in our optical system (CCD camera JAI BM-500 GE). Observe that for such bead displacement the force data used in the fittings are all within the entropic regime ($F < 10$ pN) even for the highest trap stiffness used, which justifies the use of the Marko-Siggia Worm-Like Chain (WLC) model to perform the fittings[42].

Figure 2 (*circles*) shows a typical force × extension curve obtained with the procedure above discussed for a bare λ-DNA molecule ($\sim$ 48,500 base-pairs). The *inset* shows a fitting to the Marko-Siggia Worm-Like Chain (WLC) model[42] (*solid line*). In fact, observe that the model fits very well to our experimental data, allowing us to determine the mechanical properties (persistence and contour lengths) with accuracy.

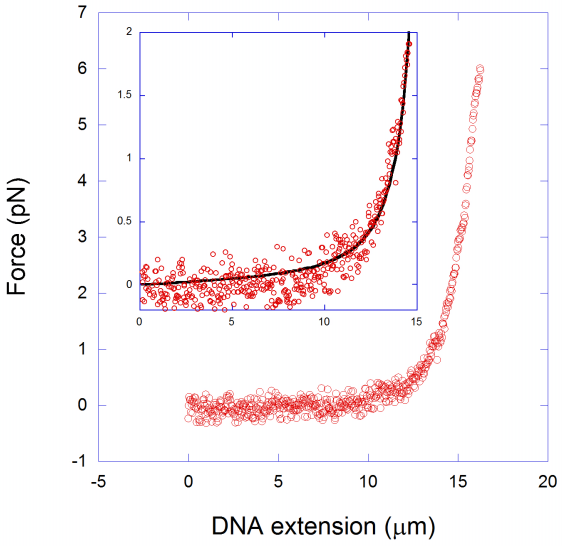

Fig. 2 Force × extension curve of a bare λ-DNA molecule in the entropic regime, with maximum force set to $\sim$ 6 pN. *Circles*: experimental data obtained with optical tweezers ($\kappa = 6.2$ pN/μm). *Solid line in the inset*: a fitting to the Marko-Siggia Worm-Like Chain (WLC) model[42].

Observe also that the data shown in Fig. 2 correspond to the case in which we have set the maximum stretching force to 6 pN ($\kappa = 6.2$ pN/μm).

More details about the sample preparation, optical tweezers setup and experimental procedure can be found in our references[15,17].

3 Results and discussion

As explained in the last section, we have performed various stretching experiments for three different values of the trap stiffness, corresponding to the maximum stretching forces F_{max} = 6 pN, 10.5 pN and 15 pN. We emphasize that these are actually the maximum forces applied to the DNA-drug complexes in all experiments, and not only trap parameters of reference. In Fig. 3 we show the persistence length (A) of DNA-doxo complexes measured as a function of F_{max}, obtained for four different doxo concentrations in the sample (2.5 μM, 3.5 μM, 4.5 μM and 5.5 μM). In this figure, and also i all subsequent ones, the dashed lines are only guides to the eye. Observe that, independent of the doxo concentration, the qualitative behavior of the experimental data is the same: the persistence length A decreases as a function of the maximum stretching force F_{max}, which shows that the measured value of this parameter obtained from single molecule stretching is

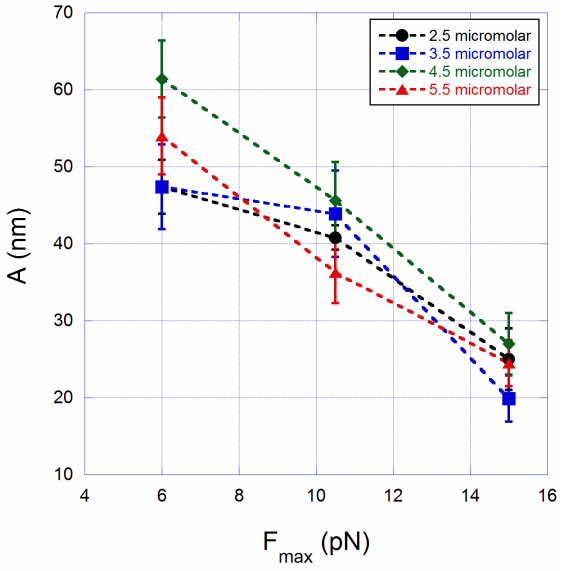

Fig. 3 Persistence length (A) of DNA-doxo complexes measured as a function of the maximum stretching force (F_{max}), obtained for four different doxo concentrations in the sample: 2.5 μM (*black circles*), 3.5 μM (*blue squares*), 4.5 μM (*green diamonds*) and 5.5 μM (*red triangles*). The dashed lines are guides to the eye.

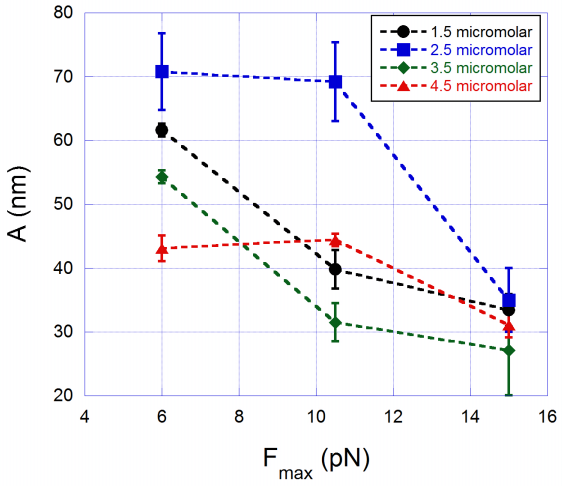

Fig. 4 Persistence length (A) of DNA-EtBr complexes measured as a function of the maximum stretching force (F_{max}), obtained for four different EtBr concentrations in the sample: 1.5 μM (*black circles*) 2.5 μM (*blue squares*), 3.5 μM (*green diamonds*) and 4.5 μM (*red triangles*). The dashed lines are guides to the eye.

strongly dependent on the force regime used to perform the experiments. On the other hand, the measured contour length L of the complexes is independent of the maximum stretching force in the regime studied here, and remains constant within the error bars when plotted as a function of F_{max}. For 2.5 μM of doxo, for example, we have found $L = (16.9 \pm 0.5)$ μm for $F_{max} = 6$ pN, $L = (16.9 \pm 0.6)$ μm for $F_{max} = 10.5$ pN and $L = (17.0 \pm 0.4)$ μm for $F_{max} = 15$ pN, corresponding to an increase of about 3% relative to the bare λ-DNA contour length (16.5 μm). For 5.5 μM of doxo, on the other hand, we have found $L = (18.9 \pm 0.6)$ μm for $F_{max} = 6$ pN, $L = (18.6 \pm 0.6)$ μm for $F_{max} = 10.5$ pN and $L = (19.1 \pm 0.7)$ μm for $F_{max} = 15$ pN, corresponding to an increase of about 14% relative to the bare λ-DNA contour length (16.5 μm).

To achieve the results reported in Fig. 3, the measurements were performed as follows. Firstly we start the experiment with only bare DNA molecules in the sample. We choose and test one of them by measuring 5 to 7 stretching curves, obtaining the mean values of the persistence and contour lengths for the bare DNA. The average results obtained were $A = (45 \pm 3)$ nm and $L = (16.5 \pm 1)$ μm, which are within the expected values for the bare λ-DNA under our experimental conditions[45–48]. Next we change the surrounding buffer solution, introducing the intercalator at a certain chosen concentration. We wait about $\sim$ 20 minutes for drug equilibration, and then repeat the stretching experiments, performing 5 to 7 measurements for each value of the trap stiffness, corresponding to the three values of the maximum stretching force cited above. These measurements were performed with the same DNA molecule in sequence of increasing F_{max}, *i. e.*, firstly we perform all the stretching measurements for $F_{max} = 6$ pN, them for $F_{max} = 10.5$ pN and finally for $F_{max} = 15$ pN. Next, we repeat the entire experiment for other different DNA molecules. The average values and error bars presented in Fig. 3 were calculated from these sets of measurements.

Figure 4 shows the same type of plot for the persistence length of the DNA-EtBr complexes, which were obtained with the same experimental procedure. Observe that the qualitative behavior of the data is the same one obtained for the DNA-doxo complexes, suggesting that such behavior is general for intercalating drugs. In addition, the contour length of the DNA-EtBr complexes is also independent of F_{max}. For 2.5 μM of EtBr, for example, we have found $L = (18.5 \pm 0.3)$ μm for $F_{max} = 6$ pN, $L = (18.8 \pm 0.5)$ μm for $F_{max} = 10.5$ pN and $L = (18.6 \pm 0.5)$ μm for $F_{max} = 15$ pN, corresponding to an increase of about 13% relative to the bare λ-DNA contour length (16.5 μm). For 4.5 μM of EtBr, on the other hand, we have found $L = (20.5 \pm 0.7)$ μm for $F_{max} = 6$ pN, $L = (20.2 \pm 0.6)$ μm for $F_{max} = 10.5$ pN and $L = (20.7 \pm 0.7)$ μm for $F_{max} = 15$ pN, corresponding to an increase of about 24% relative to the bare λ-DNA contour length (16.5 μm).

In order to guarantee that the measured effect on the persistence length is due to the intercalated drug, we also repeated the same experiment using only bare DNA molecules. The results obtained for the persistence length are shown in Fig.

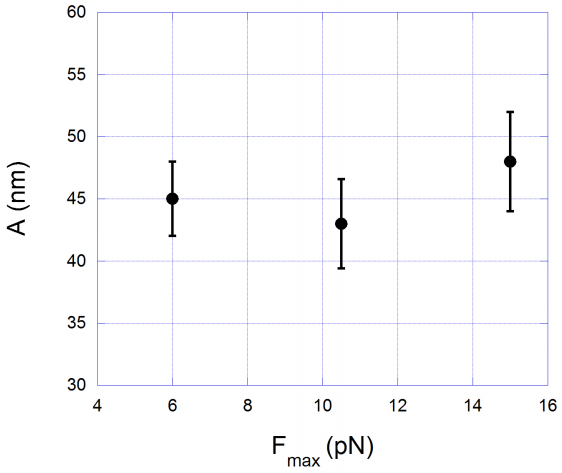

Fig. 5 Persistence length (A) of the bare DNA molecule measured as a function of the maximum stretching force (F_{max}). Observe that for the bare DNA the behavior of the persistence length is drastically different from the one observed for the DNA-intercalator complexes, being independent of F_{max}.

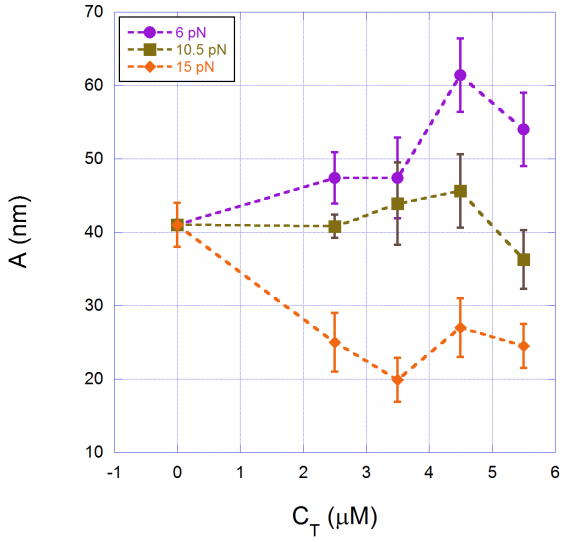

Fig. 6 Persistence length (A) of the DNA-doxo complexes as a function of the drug concentration in the sample (C_T), for the three values of F_{max} used: 6 pN (*purple circles*), 10.5 pN (*brown squares*) and 15 pN (*orange diamonds*). Observe that such behavior depends strongly on the force regime used to perform the experiments. The dashed lines are guides to the eye.

5, and the contour length is again independent of F_{max}. Observe that for the bare DNA the behavior of the persistence length is drastically different from the one observed for the DNA-intercalator complexes, being independent of F_{max} in the force regime studied here. Thus, the dependence of the persistence length on F_{max} reported here is certainly related to the strong structural perturbations that intercalators introduce on the DNA double-helix upon binding.

Before interpreting and discussing these intriguing results, it is fundamental to show again the data of Figs. 3 and 4 from a different perspective. Observe that such data can be used to plot the persistence length of the DNA-drug complexes as a function of the drug concentration in the sample, for each value of the trap stiffness. Figures 6 and 7 show such behavior, which can now be directly compared to most of the measurements found in the literature, which have monitored the persistence length of DNA-intercalator complexes as a function of drug concentration in the sample [6–8,12,13,19,20,26–37]. Observe that for the smallest trap stiffness used, corresponding to F_{max} = 6 pN, the persistence length of both DNA-doxo and DNA-EtBr complexes increases as a function of drug concentration, reaching a maximum value at a certain concentration and then decreases. Such behavior is in agreement with the results previously reported by our group for DNA complexes formed with the intercalators EtBr and daunomycin [12], psoralen [13], diaminobenzidine [19] and the bis-intercalator gelred [20]. All these works were performed with optical tweezers operating within this force regime ($F < 6$ pN). This behavior is also in agreement with results reported by other groups, as cited before [6,36,37]. On the other hand, for the highest trap stiffness used, corresponding to F_{max} = 15 pN, the persistence length exhibits an approximately monotonic decrease as a function of drug concentration, in agreement with results reported by Sischka *et al.* [7], Husale *et al.* [8], Maaloum *et al.* [26], Murade *et al.* [27], and Lipfert *et al.* [28]. Finally, for the intermediate trap stiffness used, corresponding to F_{max} = 10.5 pN, the persistence length of both complexes appears to exhibit an intermediate behavior between the two ones discussed above. It is worth to emphasize here again that the dashed lines shown in Figs. 6 and 7 are only guides to the eye.

These results lead us to conclude without doubt that the values obtained for the persistence length of DNA-intercalator complexes are strongly dependent on the applied forces used to perform the experiments. Although at first glance they may appear conflicting, these results can be understood on the basis of the following discussion. It is well known that intercalators introduce strong structural perturbations on the DNA molecule, increasing the contour length and unwinding the double-helix by a certain angle (typically 20^o to 30^o) per intercalated molecule [7,21–25]. Recently we have proposed that such perturbations distort the hydrogen bonds between the complementary base pairs in a way that partial DNA denaturation can occur even for relatively small stretching forces, with the formation of various local denaturation bubbles [12,49]. This assumption was latter confirmed by first principles density functional theory (DFT) simulations [13]. The intensity of such effect

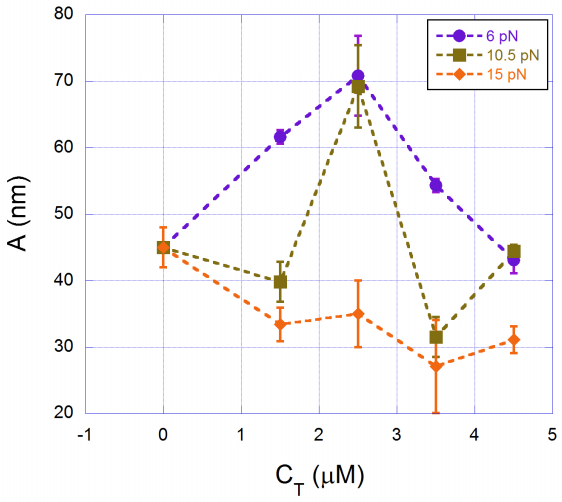

Fig. 7 Persistence length (A) of the DNA-EtBr complexes as a function of the drug concentration in the sample (C_T), for the three values of F_{max} used: 6 pN (*purple circles*), 10.5 pN (*brown squares*) and 15 pN (*orange diamonds*). Observe that such behavior depends strongly on the force regime used to perform the experiments. The dashed lines are guides to the eye.

obviously depends on the concentration of bound drug and on the force regime used to perform the stretching experiments. In fact, as the force used to stretch the DNA is increased, the probability of forming denaturation bubbles in the highly distorted double-helix of the DNA-intercalator complexes increases accordingly, thus leading to a reduction of the effective persistence length. On the other hand, if no denaturation occurs because the drug concentration is too low and/or the applied forces are sufficiently small, the persistence length of the complexes increases as a function of drug concentration. Such proposal explains why for F_{max} = 6 pN the decrease of the persistence length occurs only for relatively high drug concentrations; and for F_{max} = 15 pN we observe a monotonic decrease of this parameter. In addition, this proposal is also in agreement with an important information already mentioned in the Introduction: most works that have used non-stretching experimental techniques (viscosimetry, dynamic light scattering, fluorescence microscopy, equilibrium dialysis, etc) have found that the persistence length of DNA-intercalator complexes increases upon drug binding[29,30,32–35]. Other evidence to such result arise from experiments which have analyzed the effects of intercalators in the DNA condensation processes. It was already show that the general effect of intercalators is to prevent DNA condensation when previously bound[50–53]. From the point of view of the mechanical properties, this is an indication that the ligand in fact increases the DNA persistence length upon binding, thus increasing the energy necessary to form the pronounced bendings present in the DNA condensates[50].

Most of the contradictory results for the persistence length of DNA-intercalator complexes, otherwise, were obtained from experiments performed with typical DNA stretching techniques, such as optical and magnetic tweezers[6–8,12,13,19,20,27,28]. The AFM technique here is a case apart, firstly because it can be used as a stretching technique or as an imaging technique. When used to perform single molecule stretching, it is very similar to the tweezers and therefore present basically the same conveniences and difficulties. On the other hand, if used as an imaging technique to measure the persistence length from the conformation of the deposited DNA complexes, the method used to deposit the DNA complexes on the substrate and the substrate type itself can influence the results obtained[17,54,55].

In addition, another test can be performed to verify the partial denaturation assumption. In fact, the results presented in Figs. 6 and 7 suggest that F_{max} = 6 pN is not sufficient to induce partial denaturation for drug concentrations $\leq$ 4.5 μM for DNA-doxo complexes and $\leq$ 2.5 μM for DNA-EtBr complexes, but F_{max} = 15 pN induces such denaturation at these concentrations. Therefore, if we reverse the order of the experiments, stretching firstly with F_{max} = 15 pN, then with F_{max} = 10.5 pN and finally with F_{max} = 6 pN, the results obtained for the persistence length should all be equal for the three forces, because partial denaturation will have occurred in the first round of stretching experiments (with F_{max} = 15 pN). Figure 8 shows the results obtained with this procedure for both complexes, using one concentration of doxo (4.5 μM) and two concentrations of EtBr (2.5 μM and 3.5 μM). Observe that now the measured values of the persistence length are the same within the error bars for the three values of the trap stiffness used, thus corroborating to the interpretation of partial denaturation.

Finally, we have also performed another type of experiment that supports the partial denaturation assumption. Firstly we start stretching a DNA-drug complex with the softest trap stiffness until reaching the maximum DNA extension and then revert the velocity of the microscope stage, measuring the relaxation force $\times$ extension curve of such complex. The stretching-relaxation curve set do not exhibit any hysteresis in this case. The typical result obtained for 4.5 μM of doxo is shown in Fig. 9, where the stretching curve is represented by *green squares* and the relaxation curve is represented by *black diamonds*. Next, we repeated the experiment changing the trap stiffness during the stretching to its stiffest value approximately $\sim$ 0.5 μm before the maximum DNA extension. Now the relaxation curve (*red circles* in Fig. 9) exhibits hysteresis relative to the stretching one, indicating that some structural change on the DNA-drug complex has occurred, which is compatible to the partial denaturation assumption proposed before. In addition, if we fit the stretching and relaxation force

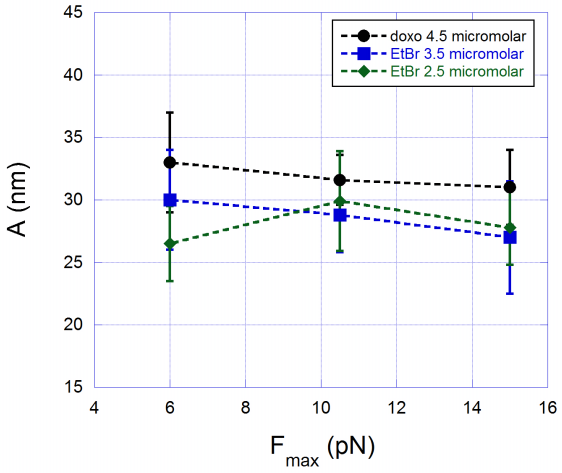

Fig. 8 Persistence length (A) of DNA-doxo complexes at 4.5 μM (*black circles*), DNA-EtBr complexes at 3.5 μM (*blue squares*) and DNA-EtBr complexes at 2.5 μM (*green diamonds*), measured as a function of the maximum stretching force (F_{max}). Here we have reverted the order of the experiments, stretching firstly with F_{max} = 15 pN, then with F_{max} = 10.5 pN and finally with F_{max} = 6 pN. The measured values of the persistence length are now the same within the error bars for the three values of F_{max}, corroborating to the interpretation of partial denaturation.

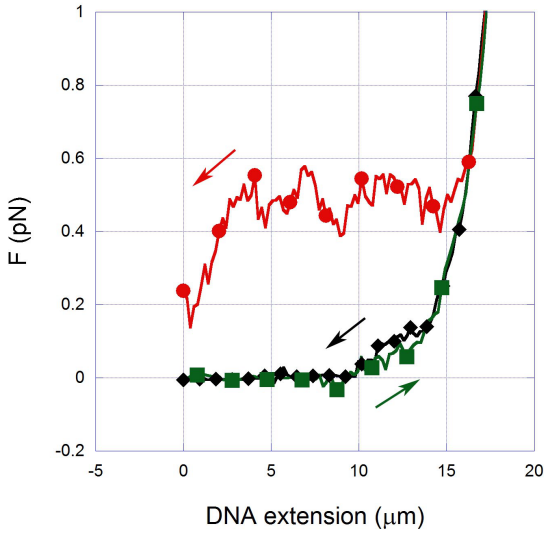

Fig. 9 Typical force × extension curves obtained by stretching and relaxing a DNA-doxo complex (4.5 μM). *Green squares*: stretching curve obtained with the softest trap stiffness; *Black diamonds*: relaxation curve obtained with the softest trap stiffness; *Red circles*: relaxation curve obtained with the stiffest trap stiffness. Observe that this last curve exhibits hysteresis relative to the stretching one, indicating that some structural change on the DNA-drug complex has occurred, which is compatible to the partial denaturation assumption.

curves to the Marko-Siggia expression, we find values of the persistence length compatible with those previously reported in Fig. 6 for the cases of F_{max} = 6 pN and F_{max} = 15 pN, respectively. This complete experiment was also repeated for bare DNA molecules, and we have not found any hysteresis in this case even when changing the trap stiffness (data not shown), which indicates that the effect is related to the presence of the intercalator.

In addition, besides the partial denaturation proposal so far discussed here, other factors can certainly influence the absolute values obtained for the persistence length of DNA-intercalator complexes measured in single molecule stretching experiments. Below we discuss the most important of these factors, which may help one to understand the discrepant results found in the literature previously mentioned.

a) Already in the original work of Marko and Siggia it was shown that the measured effective persistence length is in fact force-dependent, decreasing as the applied force on the DNA molecule increases[42]. Although such effect is not significant for the bare DNA under our experimental conditions (see Fig. 5), the effective changes introduced on the polymer chain upon intercalator binding can highlight and strengthen this effect.

b) From the physicochemical point of view, some of the results presented here can be understood assuming that the applied force changes the chemical equilibrium between the drug and the DNA molecule. Recently, Vladescu *et al.* have explicitly shown that important binding parameters such as the equilibrium association constant and the exclusion number in general depend on the force applied to the DNA-drug complexes. In particular, the equilibrium constant increases exponentially as a function of the applied force[56]. Since the equilibrium constant is closely linked to the concentration of bound drug, it is expected that the mechanical properties of the DNA-drug complexes are in fact force-dependent. For EtBr, for example it can be shown that at 6 pN the equilibrium binding constant increases about 40% in relation to the value found at zero-force. At 15 pN, such increase is about 150%[56]. Therefore, an important effect of the applied force is to increase the average amount of bound drug per DNA molecule. Another work that evidences such conclusion was recently performed by the group of F. Ritort studying bis-intercalating drugs[57]. Nevertheless, it is difficult to explain the non-monotonic behavior observed for F_{max} = 6 pN only with this assumption, since one or more binding parameters should abruptly change their values at the "critical concentration" where the persistence length invert its behavior.

c) The DNA concentration in the sample is an important parameter usually neglected in some works. In fact, it is important that the DNA concentration in the sample chamber is maintained constant during the entire experiment, because the

bound drug fraction depends strongly on the DNA concentration. In other words, the larger the DNA concentration in the sample, the larger the amount of drug that one needs to add in order to achieve saturation. Thus, for a fixed amount of drug added to the sample, the average measured mechanical properties should depend on the DNA concentration, since they depend on the bound drug fraction. This is a somewhat serious problem for sample chambers in which the DNA molecules remain free in solution and a fluid flow is applied in order to change the drug concentration, because most DNA molecules are lost during the fluid flow and therefore the bound drug fraction will saturate even for very low drug concentrations. In our sample chamber most DNA molecules remain attached to the coverslip surface, guaranteeing that the DNA concentration in the sample remains approximately unchanged during the experiment and also that a considerable amount of drug will be needed in order to achieve the bound drug saturation.

d) The experimental characteristics of each particular setup must be well known in order to avoid calibration mismatches. In particular, in Section 2.3 we have stressed that in optical tweezers experiments all bead displacements should be sufficiently small to guarantee that it is always in the harmonic region of the potential well. In magnetic tweezers experiments, on the other hand, one should pay attention to the fact that the DNA unwinding introduced by the intercalators are not propagated to the bead, which is rotationally constrained. This rotational constrain, which does not exist in optical tweezers, can lead to different results for the mechanical parameters depending on how the experiment is performed.

e) From the results discussed above it is evident that experiments performed in the enthalpic regime, with high forces (tens of pN), cannot be directly compared to those performed in the entropic regime, at least for DNA-intercalator complexes. Besides the fact that those experiments are performed in different a very different force regime, one also usually needs to use a different version of the WLC model to fit the experimental data, which includes another mechanical parameter: the stretching modulus, an enthalpic parameter related to DNA deformation due to the applied forces[58].

Finally, at this point one could ask in which force regime we should work to obtain the "correct" mechanical behavior of DNA-intercalator complexes. Probably there is not a straightforward answer to this question, since it may depend on the particular application that one intends to do with the complexes. The results presented here suggest that if one is interested in studying the mechanics of free DNA-intercalator complexes in equilibrium situations, with no external applied forces, single molecule stretching should be used only with forces as low as possible.

On the other hand, from the biological point of view, although the DNA is tightly bound to the histone proteins inside the crowded cell environment, there are theoretical and experimental evidences suggesting that the net forces acting on the DNA are on the order of a few picoNewtons[59]. These evidences suggest therefore that the experiments performed in the entropic regime are therefore closer to the *in vivo* situation. Nevertheless, the mechanical response of condensed DNA molecules is in general very different from disperse DNA molecules[50,60], and more experiments are certainly needed in order to evaluate the extension of the conclusions draw here for the *in vivo* environment.

4 Conclusion

We have performed rigorous systematic stretching experiments with two types of DNA-intercalator complexes, studying how the persistence length varies as a function of the maximum applied stretching force F_{max}. We have shown that, even in the entropic regime, the measured persistence length depends strongly on F_{max} because the applied forces can induce partial denaturation in the highly distorted double-helix structure of the DNA-intercalator complexes. These measurements clarify most of the contradictory results found in the literature on the subject, showing that single molecule stretching should be used with care to measure the persistence length of DNA-intercalator complexes. In fact, the current literature and the results presented in this work suggest that, if no stretching force is applied on the complexes and the DNA-ligand system is in equilibrium in solution, intercalators increase the DNA persistence length. Therefore, the stretching force necessary to perform single molecule stretching should be as low as possible in order to avoid disturbing the thermodynamic equilibrium and to avoid partial DNA denaturation, thus guaranteing that the persistence length measured is close to the one obtained when the complexes are not mechanically stressed.

5 Acknowledgements

This work was supported by the Brazilian agencies: Fundação de Amparo à Pesquisa do Estado de Minas Gerais (FAPEMIG), Conselho Nacional de Desenvolvimento Científico e Tecnológico (CNPq) and Coordenação de Aperfeiçoamento de Pessoal de Nível Superior (CAPES).

References

1 M. J. McCauley and M. C. Williams, *Biopolymers*, 2007, **85**, 154–168.
2 M. J. McCauley and M. C. Williams, *Biopolymers*, 2009, **91**, 265–282.
3 R. Krautbauer, L. H. Pope, T. E. Schrader, S. Allen and H. E. Gaub, *FEBS Lett.*, 2002, **510**, 154–8.
4 R. Krautbauer, S. Fischerländer, S. Allen and H. E. Gaub, *Single Mol.*, 2002, **3**, 97103.
5 R. Eckel, R. Ros, A. Ros, S. D. Wilking, N. Sewald and D. Anselmetti, *Biophys. J.*, 2003, **85**, 1968–1973.

6 I. Tessmer, C. G. Baumann, G. M. Skinner, J. E. Molloy, J. G. Hoggett, S. J. B. Tendler and S. Allen, *J. Mod. Optic.*, 2003, **50**, 1627–1636.

7 A. Sischka, K. Tönsing, R. Eckel, S. D. Wilking, N. Sewald, R. Rios and D. Anselmetti, *Biophys. J.*, 2005, **88**, 404–411.

8 S. Husale, W. Grange and M. Hegner, *Single Mol.*, 2002, **3**, 91–96.

9 K. R. Chaurasiya, T. Paramanathan, M. J. McCauley and M. C. Williams, *Phys. Life Rev.*, 2010, **7**, 299–341.

10 J. Camunas-Soler, S. Frutos, C. V. Bizarro, S. de Lorenzo, M. E. Fuentes-Perez, R. Ramsch, S. Vilchez, C. Solans, F. Moreno-Herrero, F. Albericio, R. Eritja, E. Giralt, S. B. Dev and F. Ritort, *ACS Nano*, 2013, **7**, 5102–5113.

11 J.-F. Allemand, D. Bensimon and V. Croquette, *Curr. Opin. Struc. Biol.*, 2003, **13**, 266–274.

12 M. S. Rocha, M. C. Ferreira and O. N. Mesquita, *J. Chem. Phys.*, 2007, **127**, Art. No. 105108.

13 M. S. Rocha, A. D. Lúcio, S. S. Alexandre, R. W. Nunes and O. N. Mesquita, *Appl. Phys. Lett.*, 2009, **95**, Art. No. 253703.

14 F. A. P. Crisafuli, E. C. Cesconetto, E. B. Ramos and M. S. Rocha, *Appl. Phys. Lett.*, 2012, **100**, 083701.

15 F. A. P. Crisafuli, E. C. Cesconetto, E. B. Ramos and M. S. Rocha, *Integr. Biol.*, 2012, **2012**, 568–574.

16 L. Siman, I. S. S. Carrasco, J. K. L. da Silva, M. C. Oliveira, M. S. Rocha and O. N. Mesquita, *Phys. Rev. Lett.*, 2012, **109**, 248103.

17 E. C. Cesconetto, F. S. A. Junior, F. A. P. Crisafuli, O. N. Mesquita, E. B. Ramos and M. S. Rocha, *Phys. Chem. Chem. Phys.*, 2013, **15**, 11070–11077.

18 E. F. Silva, E. B. Ramos and M. S. Rocha, *J. Phys. Chem. B*, 2013, **117**, 7292–6.

19 L. A. Reis, E. B. Ramos and M. S. Rocha, *J. Phys. Chem. B*, 2013, **117**, 14345–14350.

20 F. A. P. Crisafuli, E. B. Ramos and M. S. Rocha, *Eur. Biophys. J.*, 2015, **44**, 1–7.

21 L. D. Williams, M. Egli, Q. Gao and A. Richa, *Structure and Function - Proc. Conversation in Biomolecular Stereodynamics.*, 1992, **1**, 7th.

22 M. F. Brana, M. Cacho, A. Gradillas, B. de Pascual-Teresa and A. Ramos, *Curr. Pharmac. Des.*, 2001, **7**, 1745–1780.

23 M. K. Goftar, N. M. Kor and Z. M. Kor, *Int. J. Adv. Biol. Biom. Res.*, 2014, **2**, 811–822.

24 J. B. Chaires, N. Dattagupta and D. M. Crothers, *Biochemistry*, 1982, **21**, 3933–3940.

25 H. Fritzsche, H. Triebel, J. B. Chaires, N. Dattagupta and D. M. Crothers, *Biochemistry*, 1982, **21**, 3940–3946.

26 M. Maaloum, P. Mullera and S. Harlepp, *Soft Matter*, 2013, **9**, 11233.

27 C. U. Murade, V. Subramaniam, C. Otto and M. L. Bennink, *Biophys. J.*, 2009, **97**, 835–843.

28 J. Lipfert, S. Klijnhout and N. H. Dekker, *Nucl. Acids Res.*, 2010, **38**, 7122–7132.

29 K. E. Reinert, *Nucl. Acids Res.*, 1983, **11**, 3411–3430.

30 S. R. Quake, H. Babcock and S. Chu, *Nature*, 1997, **388**, 151–154.

31 T. Berge, N. S. Jenkins, R. B. Hopkirk, M. J. Waring, J. M. Edwardson and R. M. Henderson, *Nucl. Acids Res.*, 2002, **30**, 2980–2986.

32 K. Yoshikawa, Y. Matsuzawa, K. Minagawa, M. Doi and M. Matsumoto, *Bioch. Biphys. Res. Commun.*, 1992, **188**, 1274–1279.

33 Y. Matsuzawa and K. Yoshikawa, *Nucleos. Nucleot.*, 1994, **13**, 1415–1423.

34 G. J. Atwell, W. A. Denny, G. R. Clark, C. J. O'Connor, Y. Matsuzawa and K. Yoshikawa, *J. Phys. Org. Chem.*, 1995, **8**, 597–604.

35 Y. Matsuzawa, K. Minagawa, K. Yoshikawa, M. Matsumoto and M. Doi, *Nucleic Acids Symp. Ser.*, 1991, **25**, 131–2.

36 V. Cassina, D. Seruggia, G. L. Beretta, D. Salerno, D. Brogioli, S. Manzini, F. Zunino and F. Mantegazza, *Eur. Biophys. J.*, 2010, **40**, 59–68.

37 N. Kaji, M. U. M and Y. Baba, *Electrophoresis*, 2001, **22**, 3357–3364.

38 C. Pérez-Arnaiz, N. Busto, J. M. Leal and B. García, *J. Phys. Chem. B*, 2014, **118**, 1288–1295.

39 M. Airoldi, G. Barone, G. Gennaro, A. M. Giuliani and M. Giustini, *Biochem.*, 2014, **53**, 2197–2207.

40 J. E. Coury, L. McFail-Isom, L. D. Williams and L. A. Bottomley, *P. Natl. Acad. Sci. USA*, 1996, **93**, 12283–12286.

41 P. S. Alves and M. S. Rocha, *Appl. Phys. B*, 2012, **107**, 375–378.

42 J. F. Marko and E. D. Siggia, *Macromolecules*, 1995, **28**, 8759–8770.

43 N. B. Viana, M. S. Rocha, O. N. Mesquita, A. Mazolli, P. A. M. Neto and H. M. Nussenzveig, *Phys. Rev. E*, 2007, **75**, Art. No. 021914.

44 W. J. Greenleaf, M. T. Woodside, E. A. Abbondanzieri and S. M. Block, *Phys. Rev. Lett.*, 2005, **95**, 208102.

45 M. D. Wang, H. Yin, R. Landick, J. Gelles and S. M. Block, *Biophys. J.*, 1997, **72**, 1335–1346.

46 T. Strick, J.-F. Allemand, D. Bensimon, R. Lavery and V. Croquette, *Physica A*, 1999, **263**, 392–404.

47 S. B. Smith, L. Finzi and C. Bustamante, *Science*, 1992, **258**, 1122–1126.

48 D. Boal, *Mechanics of the cell*, Cambridge University Press, 2002.

49 M. S. Rocha, *Phys. Biol.*, 2009, **6**, Art. No. 036013.

50 M. S. Rocha, A. G. Cavalcante, R. Silva and E. B. Ramos, *J. Phys. Chem. B*, 2014, **118**, 4832–4839.

51 J. Widom and R. L. Baldwin, *Biopolymers*, 1983, **22**, 1621–1632.

52 Y. Yoshikawa, K. Yoshikawa and T. Kanbe, *Biophys. Chem.*, 1996, **61**, 93–100.

53 N. Yoshinaga, T. Akitaya and K. Yoshikawa, *Biochem. Biophys. Res. Commun.*, 2001, **286**, 264–267.

54 C. Rivetti, M. Guthold and C. Bustamante, *J. Mol. Biol.*, 1996, **264**, 919–932.

55 I. S. S. Carrasco, F. M. Bastos, M. L. Munford, E. B. Ramos and M. S. Rocha, *Mat. Sci. Eng. C*, 2012, **32**, 3639.

56 I. D. Vladescu, M. J. McCauley, M. E. Nunez, I. Rouzina and M. C. Williams, *Nat. Methods*, 2007, **4**, 517–522.

57 J. Camunas-Soler, M. Manosas, S. Frutos, J. Tulla-Puche, F. Albericio and F. Ritort, *Nucleic Acids Res.*, 2015, doi: 10.1093/nar/gkv087.

58 T. Odjik, *Macromolecules*, 1995, **28**, 7016–7018.

59 R. Blossey and H. Schiessel, *FEBS J.*, 2011, **278**, 3619–3632.

60 C. G. Baumann, V. A. Bloomfield, S. B. Smith, C. Bustamante, M. D. Wang and S. M. Block, *Biophys. J.*, 2000, **78**, 1965–1978.

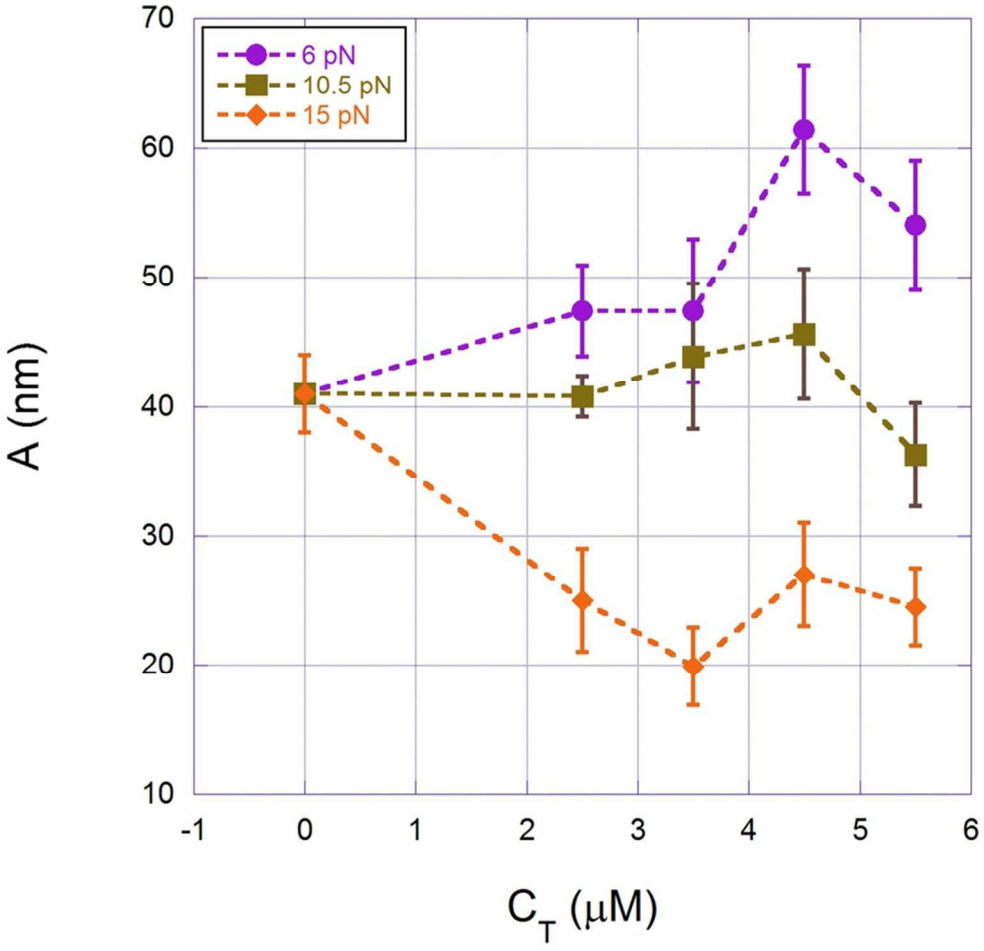

77x75mm (300 x 300 DPI)